

Multiple Nuclear Disintegrations Induced by 100-Mev X-Rays

GEORGE C. BALDWIN AND G. STANLEY KLAIBER

Research Laboratory, General Electric Company, Schenectady, New York

(Received June 20, 1946)

Multiple nuclear disintegrations have been observed in light and heavy nuclei irradiated with high energy x-rays generated by a 100-Mev betatron. 1500 photographs taken with a 12" cloud chamber filled with air have yielded 105 single protons of energies up to 9 Mev, 7 "flag" tracks showing a proton or alpha particle and a heavy recoil nucleus, and 3 four-particle "stars," in two of which one alpha-particle, two protons, and a recoil nucleus can be identified. At least one neutron must accompany the observed particles in each multiple track to satisfy the momentum conservation law. In one star, a particle which may be of intermediate mass is observed as one of the disintegration products. No recoil protons in hydrogen were observed in 150 photographs, indicating that fast

neutrons are not present in sufficient intensity to cause the observed disintegrations. Identification of residual nuclei by measurement of the half-lives of radioactivity induced in irradiated samples has revealed many multiple disintegration processes. Strong activities were observed from (γ, p) and $(\gamma, 2n)$ reactions, moderately strong activities from (γ, pn) , $(\gamma, 2p)$, and $(\gamma, 2pn)$. The reactions $Mg^{26}(\gamma, p)Na^{24}$ and $Pb^{208}(\gamma, pn)Tl^{204}$ have been established by chemical and beta-decay evidence. Weak activities were observed which could be attributed to $(\gamma, p2n)$, $(\gamma, 3pn)$, and $(\gamma, \alpha n)$ or $(\gamma, 2p3n)$. Moderately strong activities in Al and P suggest the possibility of a nuclear process induced by quanta involving the loss of charge without change of mass.

INTRODUCTION

THE successful operation of a 100-Mev betatron¹ makes possible the study of the behavior of nuclei upon excitation by quanta to energies much higher than any previously available except in the cosmic radiation. Previous studies²⁻⁵ have been confined to quantum energies below 25 Mev. The processes usually observed are (γ, γ) at low quantum energies and (γ, n) where the excitation is sufficient to expel a neutron. Approximately 35 (γ, n) reactions have been observed to date.⁶ Threshold measurements for several of these reactions have given values ranging from 1.6 Mev for beryllium to about 19 Mev for carbon.⁵ One case has been recently reported in which a (γ, p) reaction probably occurs; unfortunately this reaction leads to the formation of a previously unknown short-lived isotope and no cross check reaction or chemical test is available for confirmation.⁴

The ejection of a proton requires slightly more energy than ejection of a neutron because of the Coulomb barrier, and, as a (γ, p) reaction will not ordinarily lead to the production of a radioactive isotope, it is not so readily observable as the (γ, n) process.

At the high excitation energies now possible, the expulsion of a proton or of a neutron should be equally likely; the residual nucleus then will still be at sufficiently high temperature to evaporate several additional particles. Disintegrations in which as many as six to eight nuclear particles evaporate, including neutrons, protons and possibly alpha-particles, may be expected to follow an excitation of 100 Mev. Such disintegrations have been observed in cosmic radiation.⁷ The availability of radiation of controllable energy and intensity now permits much more complete investigations of nuclear evaporations at high energy to be made.

Though no completely satisfactory method exists for the study of multiple disintegrations which a particular nuclear species may undergo, several techniques are available. Tracks of ejected charged particles can be observed in a cloud chamber or in a photographic emulsion. Their respective energies and directions of emission can then be observed. However, this method fails to detect the neutrons emitted in the dis-

¹ E. E. Charlton and W. F. Westendorp, *J. App. Phys.* **16**, 581 (1945).

² W. Bothe and W. Gentner, *Zeits. f. Physik* **106**, 236 (1937); **112**, 45 (1939). Y. Chang, M. Goldhaber, and R. Sagane, *Nature* **139**, 962 (1937).

³ O. Huber, D. Lienhard, P. Scherrer, and H. Wäffler, *Helv. Phys. Acta* **15**, 312 (1942); **16**, 33 (1943). O. Huber, O. Lienhard, and H. Wäffler, *Helv. Phys. Acta* **17**, 195, 251 (1944).

⁴ O. Huber, O. Lienhard, P. Scherrer, and H. Wäffler, **17**, 139 (1944).

⁵ G. C. Baldwin, and H. W. Koch, *Phys. Rev.* **65**, 1 (1945).

⁶ G. T. Seaborg, *Rev. Mod. Phys.* **16**, 1 (1944).

⁷ Brode and Starr, *Phys. Rev.* **53**, 319 (1938).

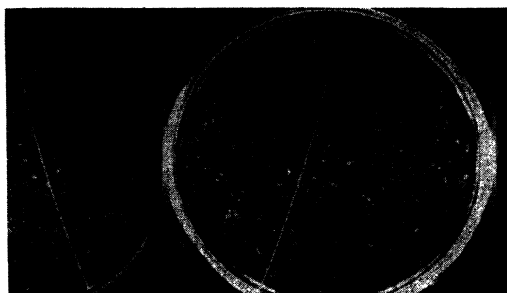


FIG. 1. The right-hand image is a direct view of the chamber; the left-hand image is a stereoscopic view obtained in a vertical mirror. Magnetic field 2650 gauss. The x-ray beam enters from the top in all photographs.

integration and thus gives only an incomplete picture of the process. Also, owing to the mixture of elements present in the cloud-chamber gas or photographic emulsion the parent element can seldom be identified with certainty. A convenient method is the observation of induced radioactivity in a sample which has been exposed to the x-ray beam. This definitely identifies the parent element and the product isotope; it does not detect reactions leading to stable end-products nor does it unambiguously identify the particular particles evaporated.

The authors have recently undertaken a program of experiments to determine what photodisintegration processes may occur and their relative probabilities, cross sections, and energy dependences, using the 100-Mev betatron of the General Electric Company as x-ray source. Experimental methods mentioned above are being employed. This program is still in its initial stage.

CLOUD-CHAMBER STUDIES

The cloud-chamber studies were made with a horizontal 12-inch chamber of $2\frac{1}{4}$ -inch depth, of which $1\frac{1}{4}$ inches were illuminated, operated once per minute in synchronism with the betatron, so that all tracks seen were of the same age and of a high degree of sharpness, as will be evident from the electron tracks visible in Figs. 3 and 4. For this work, the x-ray intensity was purposely reduced by a factor of about 10^{-5} below the full output available. The cloud chamber and the method by which it was controlled in synchronism with the operation of the betatron will be described in another publication.

The chamber was filled with air and a mixture of alcohol and water vapor at atmospheric pressure, and was located 25 feet from the x-ray target in the center of the x-ray beam. In addition to the expected electron and positron tracks, occasional tracks of heavily ionizing particles were seen. Figure 1 shows a positively charged particle moving initially at 7 degrees to the x-ray beam axis across the chamber. The magnetic field is 2650 gauss; from its curvature and ionization this particle is identified as a proton of 9 Mev kinetic energy. The short heavy track near the top of the picture crosses the chamber obliquely and thus spends only a short portion of its range in the illuminated region.

Single tracks which could be ascribed to protons were observed in about 7 percent of 1500 pictures taken with air. The majority of the single protons seen originated in the glass or brass walls of the chamber. There is no apparent asymmetry in the directions in which these particles are emitted; however, many more photographs must be taken before an accurate angular distribution can be determined.

These protons must originate in nuclear disintegrations, since no process is known by which a 100-Mev γ -ray quantum can directly transfer more than 6 Mev to a proton.

In another series of photographs, the cloud chamber was filled with hydrogen at one atmosphere. In 150 pictures, irradiating at 100 Mev, no recoil proton tracks were observed to originate in the gas of the chamber. Thus it seems unlikely that fast neutrons are present in sufficient quantity to be responsible for the disintegrations described below.



FIG. 2. Direct image on right; stereoscopic image on left. Magnetic field 2650 gauss. X-ray intensity higher than in Fig. 1.

In addition to single heavily ionizing tracks, occasional "star tracks" owing to multiple disintegrations in the gas were observed. Two-element star tracks appeared in 0.5 percent of the 1500 photographs. These "flag tracks" closely resemble photographs of disintegrations induced by fast neutrons.⁸ In all of these, one track is extremely heavily ionizing and of very short range, while the other is of longer range, usually a proton but in at least one case is definitely an alpha-particle. The direction of emission, as far as it can be determined from the few tracks observed, is random with respect to the x-ray beam. The heavier, shorter track probably is the recoil nucleus. In all these disintegrations it is necessary to assume that a neutron is also emitted in order to conserve momentum. In Fig. 2, one track is very highly ionizing and of short range, so that its direction and nature cannot be determined. The other, longer track, lies in the plane of the figure, is directed at 140 degrees to the x-ray beam direction, and stops in the illuminated portion of the chamber. Its range is 5.5

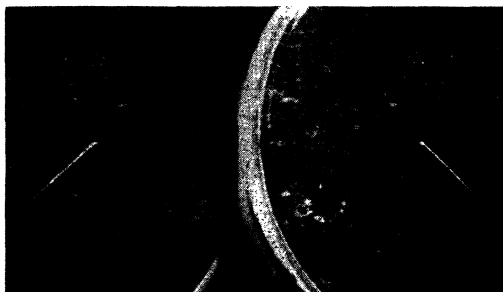


FIG. 3. Direct image on right; stereoscopic image on left. Magnetic field 1350 gauss.



FIG. 4. Direct image on left, stereoscopic on right. Magnetic field 2650 gauss.



FIG. 5. Stereoscopic views not shown. Magnetic field 1350 gauss. X-ray intensity very high.

cm. Since this shows no curvature in a field of 2650 gauss, it is probably an alpha particle with an energy of 6.8 Mev.

In Fig. 3, the shorter track ionizes very heavily. The track slopes downward at 14 degrees to the horizontal, and lies at 90 degrees to the beam direction with a range of 0.3 cm. The longer track shows a very slight curvature in the magnetic field of 1350 gauss and hence is probably a proton. It slopes upward at 16 degrees to the horizontal and its horizontal projection makes a 50-degree angle with the x-ray beam direction. It runs out of the illuminated region after traversing 6.5 cm of its range; its energy is accordingly at least 2 Mev.

Figure 4 shows a 4-element star track. The magnetic field is 2650 gauss. Track 1 is an alpha-particle of 4.9-cm range and 6.2-Mev kinetic energy. From the stereoscopic image, it can be determined that this track is inclined upward at an angle of 15 degrees with the plane of the photograph; its projection on the horizontal makes an angle of 172 degrees with the x-ray beam direction. Tracks 2 and 3 show slight positive curvature. Track 2 slopes upward at an angle of 42 degrees and passes out of the lighted volume of the chamber; its projection on the horizontal makes an angle of 62 degrees with the beam direction. The density of ionization and curvature correspond to a proton; the portion of the range

⁸ N. Feather, Proc. Roy. Soc. 136A, 709 (1932).



Fig. 6. Direct image on right. Magnetic field 1350 gauss.

visible is 3 cm so the energy is greater than 1 Mev. Track 3 is also a proton; the track slopes upward at a 25 degree angle and passes out of the illumination; the visible range is 6 cm so the energy is greater than 2 Mev. Its horizontal component makes an angle of 19 degrees with the beam direction. Track 4 is apparently the residual nucleus; its ionization is at least that of the alpha-particle and probably greater. Unfortunately it runs down at an angle of 18 ± 6 degrees and, since the star originates within 0.5 cm of the base of the illuminated region, it leaves the lighted region after approximately only 0.5 cm of its range. The angle between its horizontal projection and the beam is 20 degrees.

The star track in Fig. 5 was taken in a magnetic field of 1350 gauss. The x-ray intensity was higher than in the case of Fig. 4 and the background ionization is accordingly much higher. Track 1 is an alpha-particle of 3-cm range and 4.5-Mev kinetic energy. The track lies in the horizontal plane at an angle of 95 degrees to the beam direction. Tracks 2 and 3 are protons; track 2 slopes upward at 19 degrees and leaves the lighted region after 3.8 cm of its range; track 3 slopes upward at 42 degrees and has a visible range of 1.6 cm. The horizontal components of these tracks make angles of 20 and 10 degrees, respectively, with the beam direction. Track 4 is of at least the ionization of the alpha-particle and is probably a recoil nucleus. It may or may not end in the lighted region; the visible length is 0.3 cm. The orientation of this track is: slope, 45 degrees down; horizontal component, 162 degrees to beam axis.

Momentum cannot be conserved in either star with the tracks visible unless it is assumed that at least one neutron was also emitted in the dis-

integration. Since in each case several tracks leave the illuminated volume of the chamber and are inclined at angles too steep for reliable curvature measurement, the complete analysis of these disintegrations cannot be carried out. A reasonable assumption is that these are disintegrations of nitrogen nuclei, since the chamber was filled with air. In each star one alpha-particle and two proton tracks are observed; these carry a total of four elementary charge units. At least one neutron was emitted in each case. The fourth track would then be triply charged and hence either Li^6 or Li^7 if this interpretation is correct. The energy of the incident photon must have been at least 50 Mev in each case.

A third such star has four heavily ionizing tracks, none of which is of more than 0.5 cm range. It is not possible to identify them.

The disintegration of Fig. 6 is especially interesting. It was taken with a magnetic field of 1350 gauss. The origin of the star is in the top plane of the illuminated region. Track 1 appears to be horizontal and to stop in the gas with a range of 1.8 cm; however it is possible that it may have a slight upward slope and leaves the illumination. It makes a 67-degree angle with the beam direction. Track 2 makes a 115-degree angle with the beam direction and slopes down at 40 degrees to the plane of the photograph, leaving the base of the illuminated region after a visible range of 3.8 cm. Since the illumination is weaker at the point of origin of this star (note the apparent tapering of Track 2) it is not safe to conclude that the densities of ionization of Tracks 1 and 2 are different. Each track may be a proton or an alpha-particle. The third track

TABLE I. Values of the magnetic rigidity, $H\rho$, the range, R , and the energy E for electrons, mesons, and protons corresponding to different densities of ionization.

Density of ionization	Electron $M = m$	Meson $M = 200m$	Proton $M = 1840m$
2	$H\rho = 1.2 \times 10^3$ $R = 22$ cm $E = 0.12$ Mev	$H\rho = 2.6 \times 10^5$ $R = 3200$ cm $E = 24$ Mev	$H\rho = 23 \times 10^5$ $R = 29000$ cm $E = 230$ Mev
4	$H\rho < 10^3$ $R = 3.2$ cm $E = 0.05$ Mev	$H\rho = 1.5 \times 10^5$ $R = 750$ cm $E = 9.2$ Mev	$H\rho = 14 \times 10^5$ $R = 6900$ cm $E = 86$ Mev
8	$H\rho < 10^3$ $R < 1$ cm $E = 0.02$ Mev	$H\rho = 0.96 \times 10^5$ $R = 140$ cm $E = 3.7$ Mev	$H\rho = 8.5 \times 10^5$ $R = 1300$ cm $E = 34$ Mev

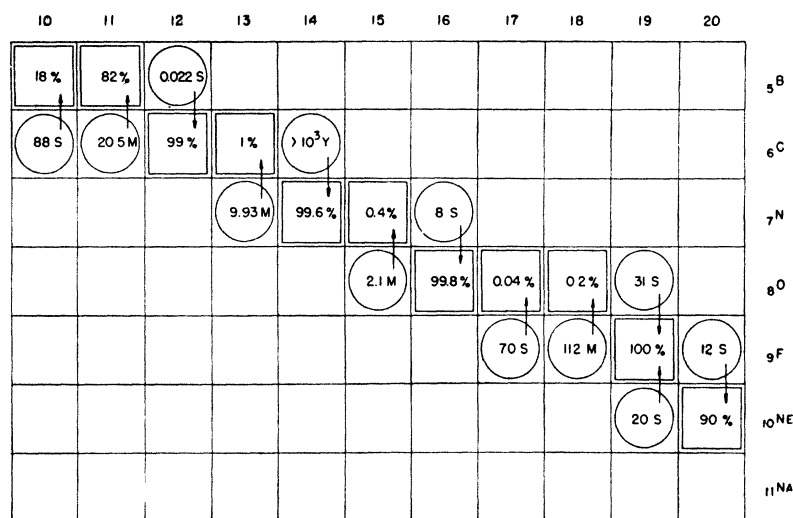


FIG. 7. Isotope chart, boron-sodium.

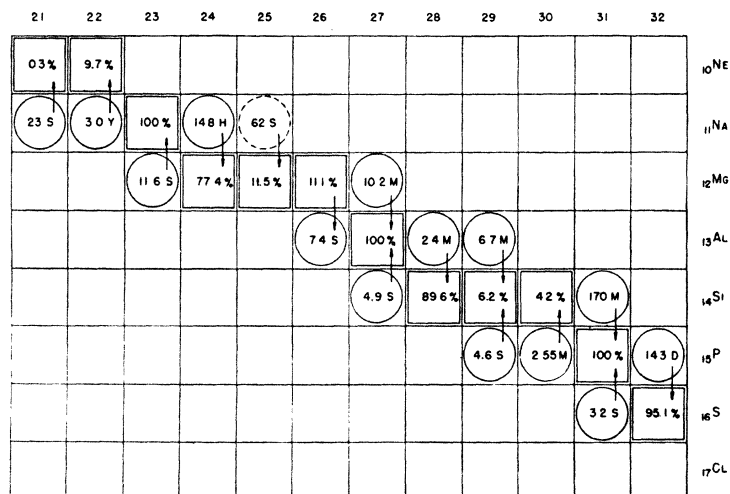


FIG. 8. Isotope chart, neon-chlorine.

runs downward at 7 degrees to the horizontal, 145 degrees to the beam. It runs out of the chamber with a range considerably more than the 12.8 cm visible. The track is considerably scattered, making a curvature measurement unreliable; however it has an apparent negative curvature with an $H\rho$ greater than 2×10^5 gauss cm. Since it traverses the fully illuminated region, its ionization can be estimated, and appears to be four times the minimum; this estimate may be high or low by a factor of two.

In Table I are listed the magnetic rigidity $H\rho$, the range R in air, and the kinetic energy E

corresponding to densities of ionization of 2, 4, and 8 times the minimum, for particles of masses 1840 (proton) and 200 (meson) times the electronic mass, and for electrons. It will be obvious from the table as well as from the pronounced scattering of the track that this cannot be an electron. A proton of ionization density 2 would have more kinetic energy than is available; even with density 4, the 86-Mev kinetic energy seems impossibly high, since it must be remembered that a neutron of approximately the same energy must be postulated to conserve momentum. If a density of 8 be ascribed to this track, it is

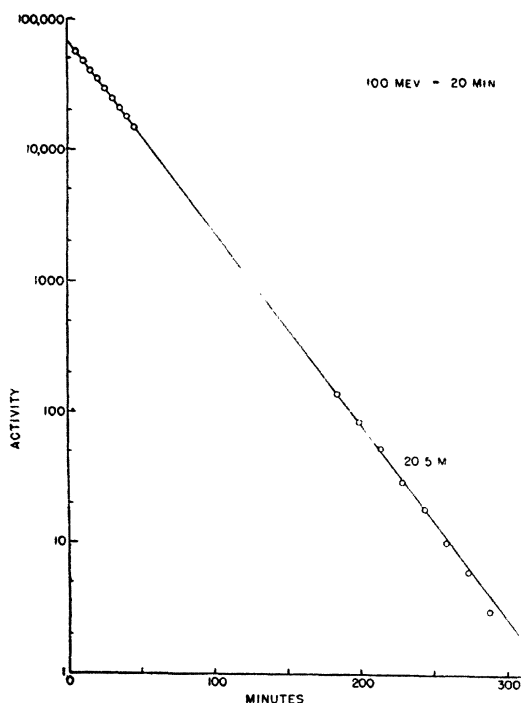


FIG. 9. Decay of carbon activity.

possible that it can be a proton. The negative $H\rho$ must then be owing to the pronounced scattering. If it is assumed that this track is owing to a particle of intermediate mass, the observed $H\rho$ is consistent with the estimated ionization and only moderate kinetic energies are involved.

INDUCED RADIOACTIVITIES

In the second method for detecting multiple disintegrations employed in the present work, samples of elements under study were exposed to the x-ray beam and then tested for induced radioactivity.

Pure elements or simple compounds of the highest purity obtainable were irradiated in the center of the x-ray beam at a standard position approximately one meter from the x-ray target of the betatron. Ordinarily irradiation was continued for one hour at 100 Mev, but in many cases other irradiation periods and electron energies were employed. The sample was then conveyed as rapidly as possible to a beta-ray counter. The latter was necessarily at a considerable distance from the irradiation point and some time was lost before the count began. This set a

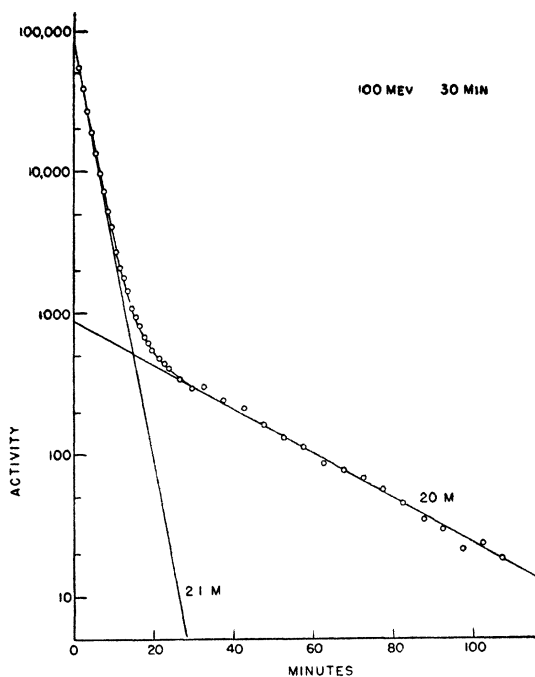


FIG. 10. Decay of boron oxide.

lower limit of 10 seconds on the half-lives which could be measured; the upper limit, set by irradiation period and x-ray intensity, was several days. The activity was followed by photographing the mechanical register and interpolator of the scaling circuit at regular intervals. From the decay curves, half-lives were determined from which active isotopes could usually be identified.⁶ In several convenient cases, chemical separations were performed⁹ to verify the assignment. Only relative estimates of intensities have been made; the x-ray intensity was not the same for all irradiations.

All but one of the elements investigated in this work were of low atomic number, in order to simplify the problem of assignment. The known stable and radioactive isotopes in this region of the elements are shown in Fig. 7 and Fig. 8.

Lithium, beryllium, and boron showed no detectable activity which could be attributed to these elements. Lithium was irradiated as the chloride, fluoride, and hydroxide; beryllium as

⁹ We are indebted to Dr. H. A. Liebhafsky, Dr. E. W. Balis, and Dr. E. W. Winslow of this laboratory for assistance with the chemical separations.

the pure metal, and boron as the carbide, nitride, and oxide. The absence of activity is to be expected, since no known isotope which might result from bombardment of these elements has a half-life within the above limits.⁶

Carbon showed a strong 20.5-minute half-life (Fig. 9). This activity is C^{11} from the reaction $C^{12}(\gamma, n)C^{11}$. Spectroscopically pure graphite and c.p. boron carbide both were tested.

Nitrogen was investigated in the forms of BN, NaN_3 , and $C_3H_6N_3$ (melamin). The decay of BN showed a strong 10-minute half-life characteristic of N^{13} and a weak activity of half-life 20 ± 2 minutes. The latter is possibly C^{11} . These activities indicate the reactions $N^{14}(\gamma, n)N^{13}$ and $N^{14}(\gamma, p2n)C^{11}$.

Oxygen was tested as boric anhydride, distilled water, and lithium and sodium hydroxides. The decay curve for boric anhydride is shown in Fig. 10. In addition to the 2.1-minute decay of O^{15} , there is a weak activity of half-life 20 ± 2 minutes which may be ascribed to C^{11} . In addition to the reaction $O^{16}(\gamma, n)O^{15}$, it is thus possible that either $O^{16}(\gamma, \alpha n)C^{11}$ or $O^{16}(\gamma, 2p3n)C^{11}$ can occur. No indication of N^{13} is apparent. It seems unlikely that the 20-minute activity is owing to contamination, as the B_2O_3 was free from carbonate; estimates of the carbon content of the H_2O and NaOH samples indicate that

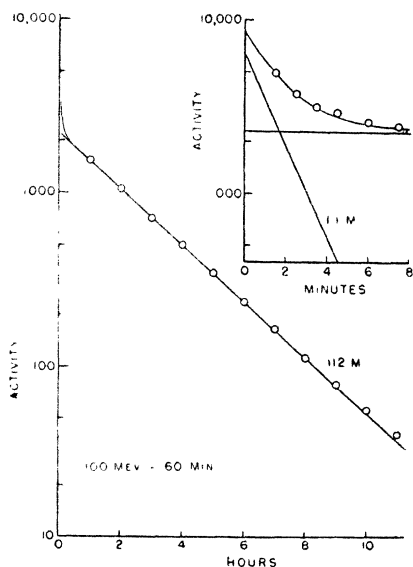


FIG. 11. Decay of sodium fluoride.

contamination will not account for the observed activity.

Fluorine was investigated as the sodium and lithium salts. The decay curve, Fig. 11, shows fairly strong 112 minute and 1.1 minute periods. The reactions occurring are $F^{19}(\gamma, n)F^{18}$ and $F^{19}(\gamma, 2n)F^{17}$.

Sodium hydroxide (Fig. 12) shows a very weak 2.2-hour activity in addition to oxygen activity. This is approximately the half-life of the F^{18} activity, and thus was masked in Fig. 11. It is possible that this is in fact F^{18} , in which case a $(\gamma, \alpha n)$ or $(\gamma, 2p3n)$ reaction must occur, as in the case of oxygen.

Magnesium was investigated as the pure metal.¹⁰ One-hour irradiation (Fig. 13) induces a complex decay curve which can be resolved into a strong 14.8-hour period, a very weak activity of half-life 40 ± 20 minutes, a strong 1-minute period and a very short period. From a 1-minute bombardment (Fig. 14), the latter two periods were found to be 62.5 seconds and 12 seconds, respectively. The 12-second activity is Mg^{23} from

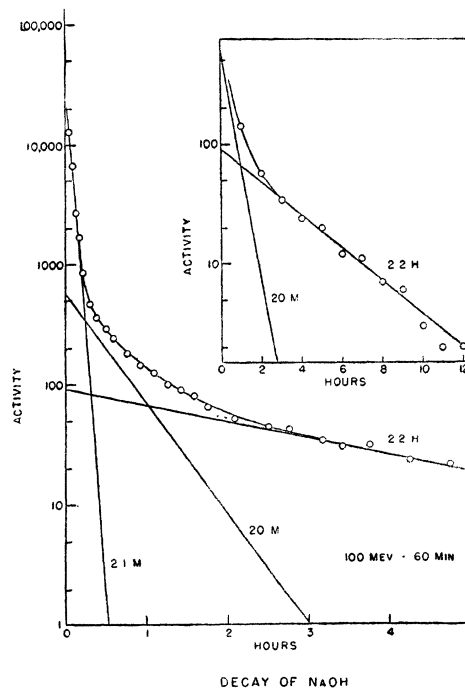


FIG. 12. Decay of sodium hydroxide.

¹⁰ Samples of spectroscopically pure magnesium were furnished us through the courtesy of the Dow Chemical Company.

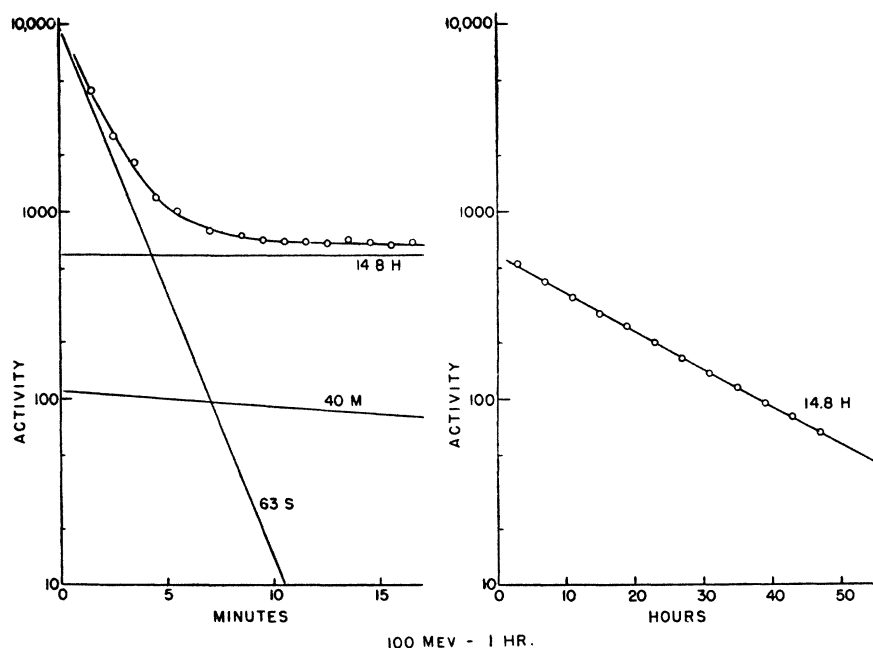


FIG. 13. Decay of magnesium—one-hour irradiation.

a (γ, n) reaction. The 62.5-second activity is the Na^{25} reported by Huber, Scherrer, Lienhard, and Waffler.³ Absorption measurements give a beta-ray end-point of 2.8 Mev, in good agreement with their value. The 14.8-hour activity emits beta- and gamma-radiations of the expected energy for Na^{24} and follows the chemistry of sodium. From this, we conclude that the reaction $\text{Mg}^{26}(\gamma, p)\text{Na}^{25}$ as well as $\text{Mg}^{25}(\gamma, p)\text{Na}^{24}$ does occur, and that the 1-minute isotope is correctly assigned. We have not yet attempted to identify the 40-minute period.

Aluminum in the form of the pure metal¹¹ showed a 14.8-hour period of moderate intensity, moderate 10-minute and 63-second activities, and a short period, probably Al^{26} from a (γ, n) reaction (Fig. 15). The 63-second and 14.8-hour periods are identical with the sodium activities obtained from magnesium, the reactions being $\text{Al}^{27}(\gamma, 2p)\text{Na}^{25}$ and $\text{Al}^{27}(\gamma, 2pn)\text{Na}^{24}$. The 10-minute activity is more difficult to explain. A rapid chemical separation showed that $\text{Mg}(\text{OH})_2$ carried the activity. It was thought that it could be Mg^{27} from an (n, p) reaction, though this re-

quires a product of cross sections. Measurements were accordingly made with silver detectors in a

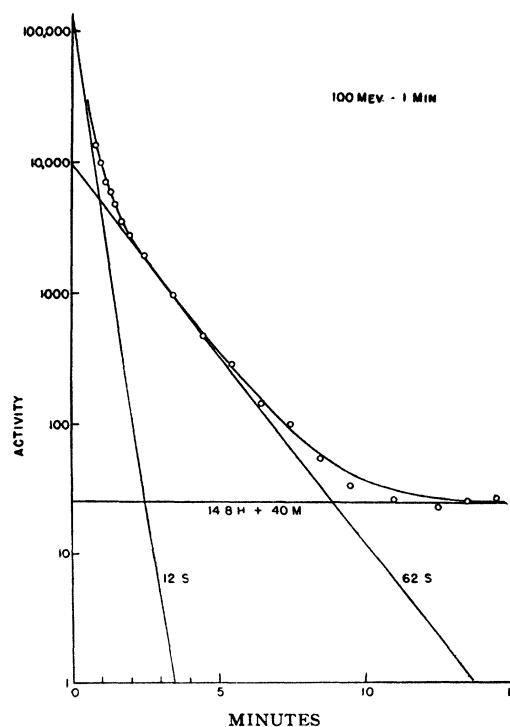


FIG. 14. Decay of magnesium—short irradiation.

¹¹ Samples of spectroscopically pure aluminum were furnished us through the courtesy of the Aluminum Corporation of America.

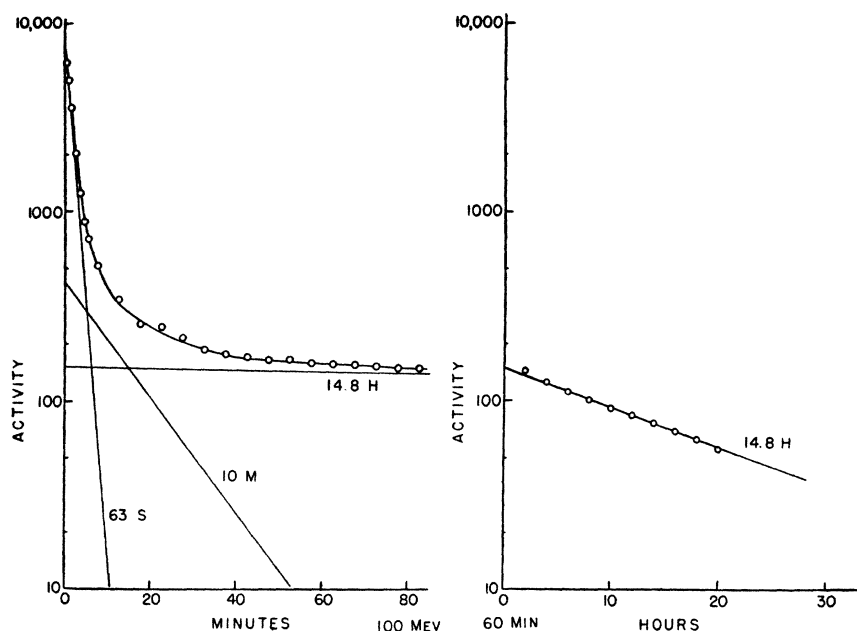


FIG. 15. Decay of aluminum.

9-inch paraffin cube to estimate the neutron intensity near the betatron. These showed only a small fast neutron background; this result is consistent with the conclusion presented earlier in this paper from the cloud-chamber studies. It was also established that an aluminum sample in the standard irradiation position did not increase this background, hence the principal source of neutrons is external to the sample. It was then shown that the 10-minute activity is produced by a radiation which is readily absorbed in lead, by simultaneously activating two aluminum samples separated by a 0.5-inch lead slab. The front sample showed approximately 50 percent more activity than the rear sample when activated at 40 Mev. This ratio is about that expected for continuous x-rays with this maximum energy¹²; neutrons should not have shown this attenuation. Attempts were also made to enhance the activity by surrounding the sample with copper and then with aluminum, without effect, while an enhancement should result if the reaction is caused by neutrons generated locally. Hence, it is probable that the re-

action is produced by quanta. Experiments are in preparation to identify the activity unambiguously and to determine the mechanism by which it is produced. Should it prove to be actually Mg^{27} , one must postulate a reaction by which a unit of charge is removed but no mass change occurs. Possible mechanisms are (1) positron emission from a highly excited state of Al^{27} ; (2) electron capture; (3) emission of a positive meson.

Silicon, also run as the pure metal, exhibited strong 2.5-minute and 6.7-minute activities and a weak 15-hour period (Fig. 16). The probable reactions are $Si^{29}(\gamma, p)Al^{28}$, $Si^{30}(\gamma, p)Al^{29}$, and $Si^{28}(\gamma, 3pn)Na^{24}$.

Phosphorus showed a long period of several days half-life, moderately strong 2.6-hour, moderately strong 6.7-minute, and strong 2.5-minute activities (Fig. 17). A very strong, short period was also observed. The latter is probably P^{29} by a $(\gamma, 2n)$ reaction. The 2.5-minute period is $P^{31}(\gamma, n)P^{30}$, though Al^{28} might also be weakly present. The 6.7-minute activity is probably from $P^{31}(\gamma, 2p)Al^{29}$. The 2.6-hour activity presents the same problem as the 10-minute activity from aluminum discussed above. No tests

¹²W. Heitler, *The Quantum Theory of Radiation* (Oxford University Press, New York, 1944), second edition.

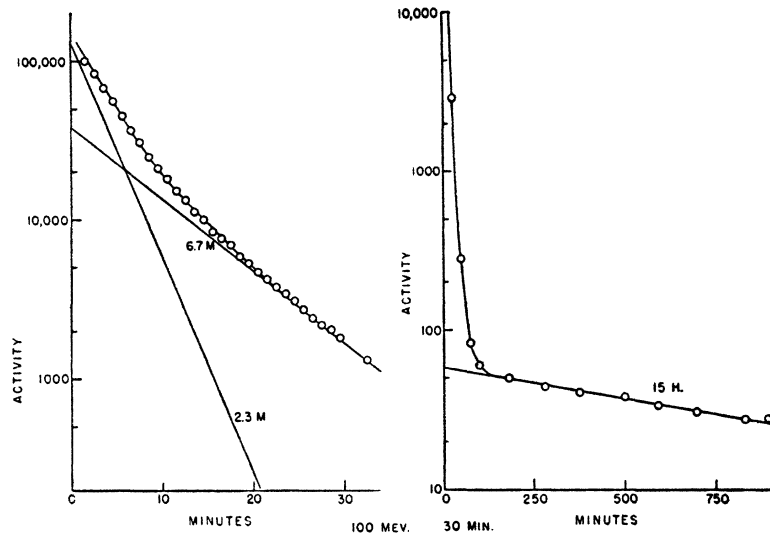


FIG. 16. Decay of silicon.

have yet been performed in this case to explore the possibility that it results from an (n, p) reaction.

Lead was also investigated, partly to ascertain

whether photo-fission can be induced to a measurable extent by high energy quanta. One-hour irradiation of spectroscopically pure lead¹³ produced the activity plotted in Fig. 18. The 69-

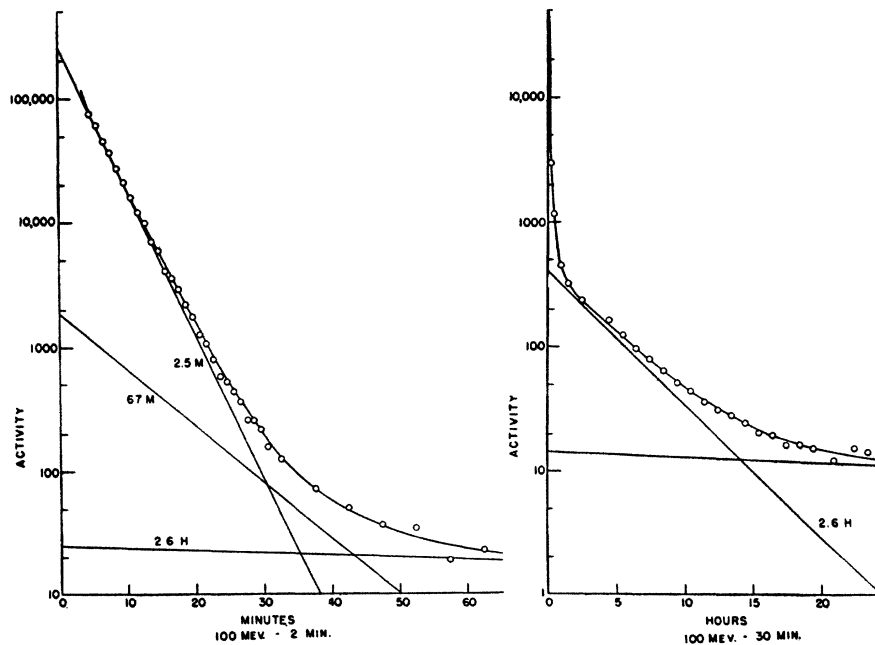


FIG. 17. Decay of phosphorus.

¹³ Samples of spectroscopically pure lead were furnished us through the courtesy of the American Smelting and Refining Company and the National Lead Company.

minute and 52-hour periods are from (γ, n) reactions. Chemical separation showed the 4.5-minute period to be thallium, hence either $\text{Pb}^{208}(\gamma, p)\text{Tl}^{207}$ or $\text{Pb}^{208}(\gamma, pn)\text{Tl}^{204}$ is indicated, or both. The maximum beta-ray energy was determined by absorption in aluminum to be 1.8 Mev. The accepted values are: Tl^{204} , 1.77 Mev; Tl^{207} , 1.47 Mev. Hence Tl^{204} is definitely present in the sample. Our best value of 4.5 ± 0.3 minutes for the half-life suggests a mixture of the activities.

The only activity remaining unassigned is the 5.5-hour activity. It seems unlikely that this single activity can be ascribed to a photo-fission product; there is no evidence that photo-fission occurs to any extent in lead which might be detectable by this method. Another experiment which confirms this conclusion will be described in a forthcoming paper.

A summary of the observed activities and probable assignments is listed in Table II.

TABLE II. Summary of activities observed and their probable assignment.

Element	Half-life	Activity	Probable isotope	Probable reaction
Li	—	—	—	—
Be	—	—	—	—
B	—	—	—	—
C	20.5 m.	strong	C^{11}	$\text{C}^{12}(\gamma, n)\text{C}^{11}$
N	9.9 m.	strong	N^{13}	$\text{N}^{14}(\gamma, n)\text{N}^{13}$
	20 m.	weak	C^{11}	$\text{N}^{14}(\gamma, p2n)\text{C}^{11}$
O	2.1 m.	strong	O^{15}	$\text{O}^{16}(\gamma, n)\text{O}^{15}$
	20 m.	weak	C^{11}	$\text{O}^{16}(\gamma, \alpha n)\text{C}^{11}?$
F	1.1 m.	strong	F^{17}	$\text{F}^{19}(\gamma, 2n)\text{F}^{17}$
	112 m.	strong	F^{18}	$\text{F}^{19}(\gamma, n)\text{F}^{18}$
Na	2 h.	weak	F^{18}	$\text{Na}^{23}(\gamma, \alpha n)\text{F}^{18}?$
Mg	12 s.	strong	Mg^{23}	$\text{Mg}^{24}(\gamma, n)\text{Mg}^{23}$
	62.5 s.	strong	Na^{25}	$\text{Mg}^{26}(\gamma, p)\text{Na}^{25}$
	40 m.	weak	?	?
Al	14.8 h.	strong	Na^{24}	$\text{Mg}^{25}(\gamma, p)\text{Na}^{24}$
	short	strong	Al^{26}	$7 \text{ s. Al}^{27}(\gamma, n)\text{Al}^{26}$
	63 s.	moderate	Na^{25}	$62 \text{ s. Al}^{27}(\gamma, 2p)\text{Na}^{25}$
	10 m.	moderate	Mg^{27}	10.5 m. ?
Si	14.8 h.	moderate	Na^{24}	$14.8 \text{ h. Al}^{27}(\gamma, 2pn)\text{Na}^{24}$
	2.5 m.	strong	Al^{28}	$2.4 \text{ m. Si}^{29}(\gamma, p)\text{Al}^{28}$
	6.7 m.	strong	Al^{29}	$6.7 \text{ m. Si}^{30}(\gamma, p)\text{Al}^{29}$
P	15 h.	weak	Na^{24}	$14.8 \text{ h. Si}^{28}(\gamma, 3pn)\text{Na}^{24}$
	short	strong	P^{29}	$4.6 \text{ s. P}^{31}(\gamma, 2n)\text{P}^{29}$
	2.5 m.	strong	P^{30}	$2.55 \text{ m. P}^{31}(\gamma, n)\text{P}^{30}$
	6.7 m.	moderate	Al^{29}	$6.7 \text{ m. P}^{31}(\gamma, 2p)\text{Al}^{29}$
	2.6 h.	moderate	Si^{31}	2.8 h. ?
Pb	4.5 m.	strong	Tl^{204}	$4.1 \text{ m. Pb}^{208}(\gamma, pn)\text{Tl}^{204}$
	69 m.	strong	Pb^{206}	$69 \text{ m. Pb}^{208}(\gamma, n)\text{Pb}^{206}$
	5.5 h.	moderate	?	?
	52 h.	strong	Pb^{208}	$52 \text{ h. Pb}^{204}(\gamma, n)\text{Pb}^{208}$

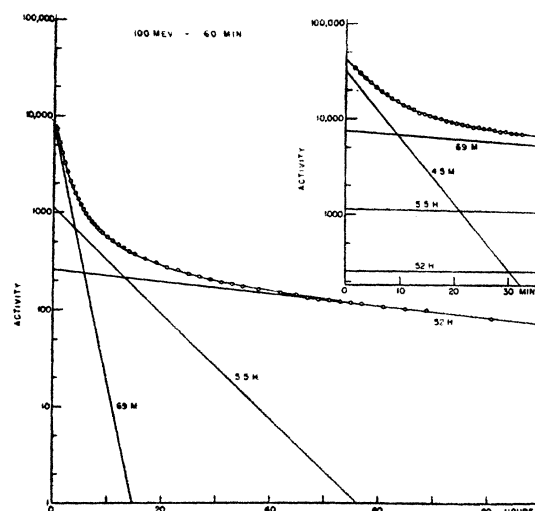


FIG. 18. Decay of lead.

DISCUSSION

The experiments described demonstrate that excitation of nuclei by 100-Mev x-rays will lead to the evaporation of as many as four or more particles of moderate energies including neutrons, protons, alpha-particles, and possibly charged particles of intermediate mass.

It must be remembered that by "100-Mev x-radiation" is meant the *continuous* spectrum of x-rays generated by the bremsstrahlung of 100-Mev electrons in a thin tungsten target and that this radiation has emerged through the walls of the glass vacuum tube. The spectral distribution of this radiation has not yet been determined experimentally; however, quanta of all energies up to 100 Mev should be present¹² and the disintegrations observed are undoubtedly owing chiefly to quanta of energies well below 100 Mev.

The experimental methods which have so far been available for the study of these processes do not give a complete account of the possible modes of disintegration of a given nucleus under study. Few of the residual nuclei will in general be radioactive with lifetimes convenient for rapid study; stable products should be expected to be slightly more probable than unstable ones. The method of induced radioactivity will however permit accurate measurement of relative probabilities of various modes of disintegration and will be especially useful when applied to

separated isotopes. As soon as projected experiments to determine the spectrum and to count absolutely the density of quanta in the x-ray beam have been completed, it will be possible to measure excitation functions and absolute cross sections for these disintegration processes.

ACKNOWLEDGMENT

The authors sincerely appreciate the enthusiastic support of Dr. W. D. Coolidge and Dr. E. E. Charlton, and the invaluable assistance of Mr. W. F. Westendorp in the solution of many technical problems.

PHYSICAL REVIEW VOLUME 70, NUMBERS 5 AND 6 SEPTEMBER 1 AND 15, 1946

The Paths of Ions and Electrons in Non-Uniform Crossed Electric and Magnetic Fields*

NORMAN D. COGGESHALL

Gulf Research and Development Company, Pittsburgh, Pennsylvania

(Received December 8, 1945)

The integration of the force equations for a charged particle moving in the presence of particular types of crossed, non-uniform, electric, and magnetic fields is shown to be possible in a very simple manner. The cases which admit of the integration are those such that: the magnetic field is a function of only one coordinate (either Cartesian or the radius vector in a polar system); the electric field is a function of only one coordinate which for any particular case is the same coordinate with which the magnetic field varies; the electric field has a component only in the direction of the variable with which it varies; and the two fields are orthogonal. Since these conditions, in most cases, are only met on a median plane symmetrically situated relative to magnetic pole faces and electrostatic electrodes, the calculations refer to the motion in this plane. The equations are solved and discussions made of the orbits for several different field arrangements and for one a new type of perfect focusing. The method can be used with numerical integration when the analytical difficulties are too great or when the fields are only known empirically.

INTRODUCTION

THE integration of the Lorentz force equation for charged particles moving in the presence of certain types of non-uniform magnetic fields has been reported earlier.¹ The cases dealt with were those such that the magnetic field varied as a function of one coordinate only, either Cartesian or the radius in cylindrical or polar coordinates; the motion of the charged particles was in a plane perpendicular to the magnetic field (this in some cases restricts the motion to the median plane between the pole faces of a magnet or electromagnet); and there was no electric field present. This integration was of such a nature that it could be done analytically if the functions were simple enough

or, if not, it could always be done numerically to as fine an accuracy as desired. Furthermore, for cases where the magnetic field was known only experimentally, the integration could be done numerically to an accuracy equal to that of the data. Several cases of focusing were reported, some of which do not correspond to anything obtainable with uniform fields.

In the present paper the method of integration has been extended to cover certain cases of combined magnetic and electric fields which may or may not be uniform. The restrictions are: The magnetic field is constant or is a function of only one coordinate (either Cartesian or the radius vector in spherical or cylindrical coordinates); the electric field is constant or a function of only one coordinate which for any particular crossed field arrangement is the same coordinate with which the magnetic field varies; the electric and magnetic fields are perpendicular to each

* An abstract of a preliminary report is given in *Phys. Rev.* **68**, 98 (1945).

¹ N. D. Coggeshall and M. Muskat, *Phys. Rev.* **66**, 187 (1944).

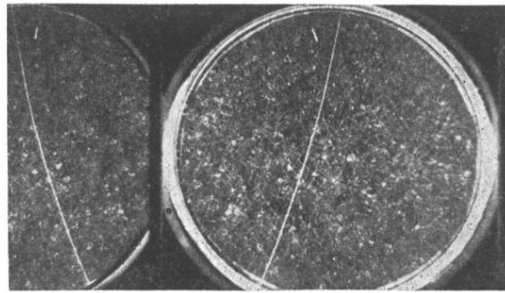


FIG. 1. The right-hand image is a direct view of the chamber; the left-hand image is a stereoscopic view obtained in a vertical mirror. Magnetic field 2650 gauss. The x-ray beam enters from the top in all photographs.

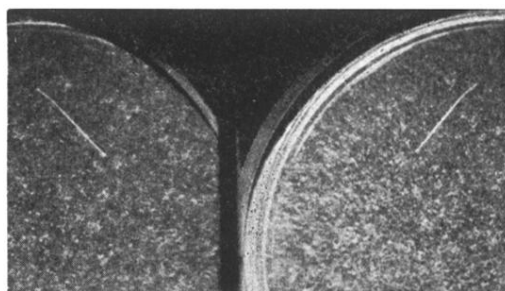


FIG. 2. Direct image on right; stereoscopic image on left. Magnetic field 2650 gauss. X-ray intensity higher than in Fig. 1.

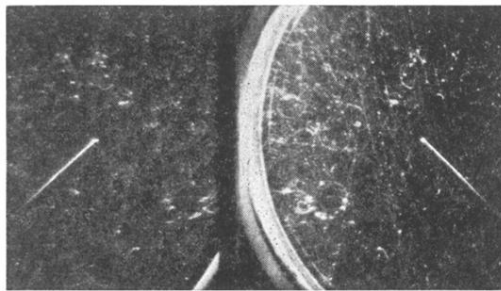


FIG. 3. Direct image on right; stereoscopic image on left. Magnetic field 1350 gauss.

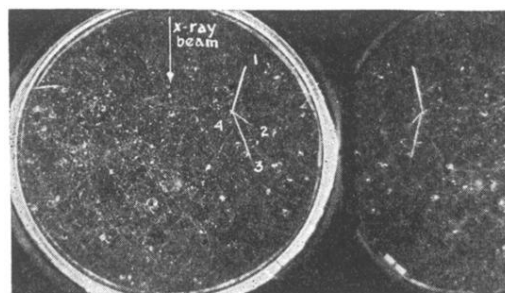


FIG. 4. Direct image on left, stereoscopic on right. Magnetic field 2650 gauss.

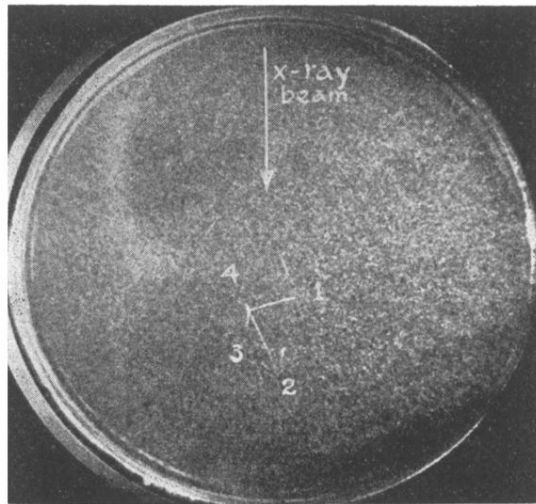


FIG. 5. Stereoscopic views not shown. Magnetic field 1350 gauss. X-ray intensity very high.

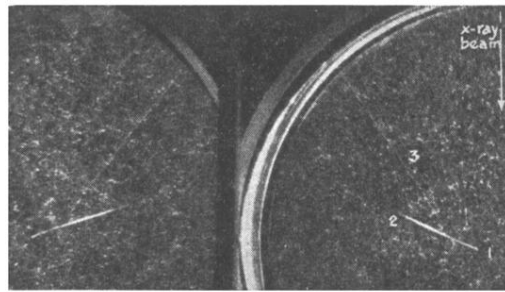


FIG. 6. Direct image on right. Magnetic field 1350 gauss.